Chronic CD30-signaling in B cells results in lymphomagenesis by driving the expansion of plasmablasts and B1 cells

Stefanie Sperling[1*], Petra Fiedler[1*], Anna Pollithy[1], Markus Lechner[1], Stefanie Ehrenberg[1], Ana-Iris Schiefer[2], Lukas Kenner[2,3,6,7], Annette Feuchtinger[4], Ralf Kühn[5], Lothar J. Strobl[1*] and Ursula Zimber-Strobl[1*]

[1]Research Unit of Gene Vectors, Helmholtz Center Munich, German Research Center for Environmental Health GmbH, Munich, Germany
[2]Department for Experimental and Laboratory Animal Pathology, Medical University Vienna, Vienna, Austria
[3]Ludwig Boltzmann Institute for Cancer Research, Vienna, Austria
[4]Research Unit Analytical Pathology, Helmholtz Zentrum München, Neuherberg, Germany
[5]Max Delbrück Center for Molecular Medicine, Berlin-Buch, Germany.
[6]Unit of Pathology of Laboratory Animals, University of Veterinary Medicine Vienna, Vienna, Austria.
[7]CBMed Core Lab2, Medical University of Vienna, Vienna, Austria
*these authors contributed equally

Corresponding author:

Ursula Zimber-Strobl

Research Unit of Gene Vectors

Helmholtz Center Munich

Marchioninistrasse 25

81377 Munich

Germany

E-mail: strobl@helmholtz-muenchen.de

phone: +49-3187-1523

fax: +49-3187-1225

Running title: Chronic CD30-signaling in B lymphocytes

Section: lymphoid neoplasia

word counts: text: 3,973, abstract: 246, figure/table count: 7, reference count: 48

Key points:

- CD30-signaling drives the expansion of B1 cells and plasmablasts/plasma cells in transgenic mice.
- Chronic CD30-signaling in murine B cells results in the development of B-cell lymphomas.

Abstract

CD30 is expressed on a variety of B-cell lymphomas such as Hodgkin's lymphoma, primary effusion lymphoma, and a subgroup of diffuse large B-cell lymphoma. In normal tissues, CD30 is expressed on some activated B and T lymphocytes. However, the physiological function of CD30-signaling and its contribution to the generation of CD30-positive lymphomas are still poorly understood. To gain a better understanding of CD30-signaling in B cells, we studied the expression of CD30 in different murine B-cell populations. We show that B1 cells express higher levels of CD30 than B2 cells and that CD30 is upregulated in $IRF4^+$ plasmablasts (PB). Furthermore, we generated and analyzed mice expressing a constitutively active CD30-receptor in B lymphocytes. These mice displayed an increase of B1 cells in the peritoneal cavity (PerC) and in secondary lymphoid organs as well as increased numbers of plasma cells (PC). TI-2-immunization resulted in a further expansion of B1 cells and PC. We provide evidence that the expanded B1 population in the spleen includes a fraction of PB. CD30 signals appeared to enhance PC-differentiation by increasing activation of NF-κB, higher levels of phosphorylated STAT3 and STAT6 and of nuclear IRF4. In addition, chronic CD30-signaling led to B-cell lymphomagenesis in aged mice. These lymphomas were localized in the spleen and PerC and had a B1-like/plasmablastic phenotype. Our mouse model most likely mirrors chronic viral infections or autoimmune diseases with increased numbers of $CD30^+$ lymphocytes and provides experimental proof that chronic CD30-signaling increases the risk of B-cell lymphomagenesis.

Introduction

CD30 is a member of the tumor necrosis factor receptor (TNF-R) superfamily[1]. Initially, CD30 was defined as a marker of Hodgkin's lymphoma [2] but was later also detected on non-Hodgkin lymphomas (NHL) including anaplastic large-cell lymphomas[3], primary effusion lymphomas (PEL)[4,5], and a subgroup of diffuse large B-cell lymphomas (DLBCL)[6,7]. In addition, CD30 is expressed on virally infected lymphocytes including Epstein–Barr virus (EBV)-infected B cells or human immunodeficiency virus (HIV)-infected T cells as well as on lymphocytes of patients suffering from autoimmune diseases[8]. Elevated levels of soluble CD30, that arise from the extracellular cleavage of CD30, are often detectable in the sera of patients with $CD30^+$ lymphomas and chronic infections[1,9]. CD30 and its ligand CD30L were cloned over two decades ago[10-13], but the role of CD30-signaling in B lymphocytes is still poorly understood. Previous studies reported that upregulation of CD30 in human B cells by CD40-stimulation inhibited class switch recombination and immunoglobulin secretion[14], whereas in murine B cells CD30-stimulation enhanced immunoglobulin secretion[15]. Also studies in CD30 knock-out (CD30ko) mice did not reveal a clear function of CD30-signaling in B cells[16]. CD30ko mice had a defect in sustaining germinal center (GC) responses and inducing secondary immune responses; however, this defect was attributed to the impaired generation of $CD4^+$ memory T cells[17]. No studies have investigated whether CD30-deficient B cells also contribute to this phenotype. Similarly, although CD30 is highly expressed on several B-cell lymphomas, it is unclear whether deregulated CD30-signaling actively drives B-cell lymphomagenesis. Because $CD30^+$ lymphomas are often correlated with viral infections, including EBV, Kaposi´s sarcoma-associated herpesvirus (KSHV) and HIV[18], there might be a correlation between chronic immune stimulation and the development of $CD30^+$ lymphomas. This hypothesis was strengthened by recent cohort studies showing that elevated levels of soluble CD30 in immunocompetent healthy persons were associated with an increased risk of developing NHL[19-23].

To study the role of CD30-signaling in B-cell activation and lymphomagenesis, we generated a new transgenic mouse strain (LMP1/$CD30^{flSTOP}$ mice) expressing a constitutive active CD30-receptor upon Cre-mediated recombination. We demonstrated that B cell-specific expression of LMP1/CD30 leads to the expansion of

B1 cells and increased plasma cell (PC) numbers. Furthermore, we provide evidence that chronic CD30-signaling results in lymphoma development.

Methods

Mice

The LMP1/CD30-transgene was inserted together with a loxP flanked stop-cassette into the *Rosa26*-locus of embryonic stem (ES) cells. Chimeric mice were obtained from the microinjection of ES cells into blastocysts and used to establish the LMP1/CD30^{flSTOP} transgenic mouse line. For the B cell-specific expression of LMP1/CD30 we used CD19-Cre mice[24]. R26/CAG-CARΔ1^{StopF} reporter mice were kindly provided by Marc Schmidt-Supprian and Cγ1-Cre mice by Stefano Casola[25,26]. Mice were analyzed on a BALB/c background. Mice were bred and maintained in specific pathogen-free conditions and experiments were performed in compliance with the German Animal Welfare Law and were approved by the Institutional Committee on Animal Experimentation and the government of Upper Bavaria.

Cell purification

B cells were isolated from splenic cell suspensions using CD43-Micro Beads or a Pan-B cell Isolation Kit (Miltenyi-Biotec, Bergisch-Gladbach, Germany) according to the manufacturer's instructions (MACS-separation). B1 (CD23^{low}CD43^{+}) cells and B2 (CD23^{+}CD43^{-}) cells were sorted with a BD FACSAria™III.

Protein detection

Whole cell extracts were prepared with NP40 lysis buffer. Nuclear and cytoplasmic extracts were generated with the NE-PER Kit (ThermoScientific, Waltham, MA, USA). Western blot analyses were performed as described previously[27] or with the WES system, a fully automated Western blot system (ProteinSimple, San Jose, CA, USA), according to the manufacturer's instructions. (additional information in supplemental methods).

In vitro cultures

In vitro culture conditions are described in supplemental methods.

Flow Cytometry

All FACS antibodies were purchased from BD Biosciences (Heidelberg, Germany) except for the CAR-antibody (Santa Cruz Biotechnology, Dallas, TX, USA).
For intracellular FACS-stainings, cells were fixed with 2% paraformaldehyde (PFA) and permeabilized with methanol. Analysis was performed with a FACSCalibur (BD Biosciences) or LSRFortessa (BD Biosciences). Results were analyzed with FlowJo Version 10 (TreeStar) software.

Histology

Immunohistochemistry was performed by using OCT (VWR Chemicals, Radnor, PA, USA) or paraffin embedded tissues. Further information is given in supplemental methods.

Statistics

Two-tailed Student *t*-test was used to determine the significance of splenic weight values, percentages of FACS analyzed cell populations, and calculated absolute cell numbers. Because of their lognormal distribution, immunoglobulin titers were logarithmized prior to determining significant differences between two genotypes using the two-tailed Student *t*-test. *P ≤ 0.05, ** P ≤ 0.01 *** P ≤ 0.001, and ****P ≤ 0.0001. All statistical calculations were performed using Prism 7 (GraphPad Software).

Results

Expression of CD30 on murine B cells

We examined CD30-surface expression on different mature B-cell populations, and after *in vitro* activation. In the PerC, B1 cells expressed more CD30 than B2 cells with slightly higher levels in B1a than B1b cells. These expression differences were also observed in splenic B cells but to a lower extent (Figure 1A, supplemental Figure 1A).

This was in accordance with *in silico* data revealing CD30 mRNA expression was higher in B1a and B1b cells compared with B2 cells in the PerC and was slightly increased in B1a compared with B2 cells (follicular B cells (FoB) and marginal zone B (MZB) cells) in the spleen (Figure 1B). *In vitro*, CD30 was most upregulated by CD40/IgM-co-stimulation, whereas LPS-, CD40- or IgM-stimulation resulted in a weaker upregulation (Figure 1C, supplemental Figure 1B). CD40/IgM-co-stimulation resulted in a stronger upregulation of CD30 on B1 compared to B2 cells (supplemental Figure 1C). *In silico* analysis revealed upregulation of CD30 mRNA in blasts and plasmablasts (PB) (Figure 1D). Furthermore, CD30 was upregulated in splenic $IRF4^+$ PB/PC compared with $IRF4^-$ splenic B cells (Figure 1E) in accord with the co-expression of CD30 and IRF4 by some human tonsillar lymphocytes[28]. Therefore, CD30 is upregulated in B1 cells relative to B2 cells, upon PC-differentiation and mitogenic stimulation.

Generation of the conditional transgenic mouse strain LMP1/CD30^{flSTOP}

To study the function of CD30 in B-cell activation and lymphomagenesis, we generated mice conditionally expressing a constitutive active CD30-receptor. We cloned a LMP1/CD30-fusion gene consisting of the transmembrane domain of the EBV latent membrane protein 1 ($LMP1^{TM}$) and the intracellular signaling domain of CD30. LMP1/CD30 exerts ligand independent CD30-signaling by self-aggregation of $LMP1^{TM}$ in the plasma membrane. We already demonstrated the efficacy of this approach by generating a constitutive active CD40-receptor[27,29]. The functionality of the LMP1/CD30-fusion protein was verified by a NF-κB dependent luciferase activity assay in HEK293 cells after transient transfection with an LMP1/CD30-expression-construct (supplemental Figure 2A). The transgene was inserted together with a loxP flanked stop-cassette into the *rosa26*-locus. After removal of the stop-cassette by Cre, the LMP1/CD30 was expressed under the control of the *rosa*26-promoter together with the reporter gene hCD2 (supplemental Figure 2B).

Constitutive CD30-expression in B cells leads to the expansion of B1 cells

In all analyses we used mice that were heterozygous for LMP1/CD30 and CD19-Cre, designated LMP1/CD30 hereafter. Controls were mostly CD19-Cre$^{+/-}$ mice. In some cases, CD19-Cre$^{+/-}$ were replaced by LMP1/CD30$^{flSTOP/wt}$ or wildtype mice. Deletion efficiency of the stop-cassette was low in developing B cells of the BM but reached more than 94% in mature B cells (supplemental Figure 3A+B). LMP1/CD30-protein from splenic B lymphocytes was detected at a size of around 54 kDa (supplemental Figure 3C).

LMP1/CD30-mice revealed splenomegaly and displayed significantly increased B-cell numbers in the spleen compared with controls, whereas T-cell numbers were comparable (Figure 2A). Histology of the spleen revealed a normal follicle structure with a B and T cell zone surrounded by a MZ. However, more B cells expressing high levels of IgM were located in the red pulp compared with control sections (Figure 2B). LMP1/CD30-mice displayed a significant expansion of B cells with the phenotype IgM^{+}IgD^{low}CD21^{low}CD23^{low}CD43^{+}B220^{low}, and either CD5^{+} or CD5^{-} in accord with B1a- and B1b-cell phenotypes (Figure 2C). An increased percentage of B1 cells was also detected in lymph nodes (LN) and blood (supplemental Figure 4A+B). In the PerC, total lymphocyte numbers were increased (supplemental Figure 4C) with a 4–5-fold increase in B1a- and B1b-cell numbers (Figure 2D).
Thus, constitutive CD30-signaling results in the expansion of peripheral B lymphocytes with mostly a B1-cell phenotype.

Constitutive CD30-signaling enhances PC-differentiation

The upregulation of CD30 in PB (Figure 1D) suggests a role for CD30-signaling in PC-differentiation. Indeed, the percentages of PCs were increased in the spleen and BM of LMP1/CD30-mice (Figure 3A) resulting in elevated total IgM-, IgG2a-, IgG3- and IgA-antibody titers in the serum (Figure 3B). *In vitro* PB generation as well as IgM secretion was enhanced in the absence and presence of LPS-stimulation in cultures of LMP1/CD30^{+} B cells in comparison to controls (supplemental Figure 5A-C). Analysis of the expression levels of Blimp1 (Prdm1), IRF4, and Xbp1, which are upregulated, and Pax5, which is downregulated during PC-differentiation[30] revealed that splenic B1 cells of both genotypes had higher Prdm1 and Xbp1 and lower Pax5

levels of mRNA than B2 cells (Figure 3C). Prdm1 mRNA levels had a tendency to be increased and IRF4-protein levels were higher in B1 cells of LMP1/CD30-mice compared with controls (Figure 3C-D). Furthermore, the percentage of $CD138^+$ cells within the B1 cell fraction was higher in LMP1/CD30-mice than in controls (Figure 3E). Also after depletion of $CD138^+B220^{low}$ cells, LMP1/CD30-expressing B1 cells were able to differentiate to PB without further stimulation (Figure 3F) indicating that LMP1/CD30 is sufficient to drive PC-differentiation of B1 cells.

LMP1/CD30-expressing B2 cells did not spontaneously differentiate to PB *in vitro* (Supplemental Figure 7A+B). However, PC-differentiation was enhanced upon CD40-stimulation in comparison to controls (Figure 4A). Interestingly, CD40-stimulation of B2 cells resulted in the generation of $CD23^{low}CD43^+$ cells and the percentage of this population was higher in LMP1/CD30- compared to control B cells (Figure 4B). In both genotypes the $CD23^{low}CD43^+$ population contained a fraction of $CD138^+$ cells (Figure 4C), expressed higher levels of CXCR4, and lower levels of CD22 (Figure 4D) in accord with a plasmablastic phenotype[31]. Therefore, the expanded $CD23^{low}CD43^+$ population in LMP1/CD30 mice may consist of a mixture of expanded B1 cells and PC-progenitors. PB could originate either from B1 cells spontaneously or from CD40-stimulated B2 cells. As shown by *in silico* analysis, most of the surface markers are similarly expressed in PC progenitors and B1 cells but some markers such as CXCR4 are differentially expressed allowing the discrimination of PB and B1 cells (Supplemental Figure 8).

We detected higher pSTAT3, pSTAT6, as well as p65 and IRF4 levels in the nuclear fractions of CD40-stimulated LMP1/CD30-expressing splenic B2 cells compared with controls (Figure 4E-G). Interestingly, phosphorylation of STAT3 has a crucial role in PC-differentiation by upregulating BLIMP1[32,33], and IRF4 is a known NF-κB target gene[34]. We conclude from these data that CD30-signaling in cooperation with other signals such as CD40 increases pSTAT6 and pSTAT3 levels as well as nuclear translocation of NF-κB components, resulting in the enhanced upregulation of IRF4 and BLIMP1.

LMP1/CD30 enhances the generation of splenic B1a cells and PCs upon TI-2-immunization.

Based on our *in vitro* data, we assumed that CD30-signaling enhances antibody secretion during immune responses. To investigate this, we immunized mice with the TI-2 antigen NP-Ficoll, which B1 and MZ B cells respond to. Immunization resulted in a further increase in the percentages of total PCs and B1a cells in LMP1/CD30-mice but not in controls (Figure 5A). NP-specific IgM and IgG3 PCs in the spleen were increased in LMP1/CD30-mice in comparison with controls (Figure 5B). Moreover, NP-specific IgM-antibody titers were higher in the serum of immunized LMP1/CD30-mice related to controls (Figure 5C). These data showed that CD30-signaling enhances the TI-2 Ab response to NP-Ficoll and results in a further expansion of B1a cells. To analyze whether CD30-signaling has the same effect during TD-immune responses, we immunized mice with the TD-antigen NP-CGG.

In contrast to controls the formation of GCs was strongly decreased in LMP1/CD30-mice (Figure 5D, supplemental Figure 9A). Decreased percentages of GC B cells were also observed in Peyer´s patches (PP), where GCs are continuously generated independent of immunization (supplemental Figure 9B). Moreover, the percentages of $hCD2^+$ B cells were lower in GC than in non-GC B cells suggesting a counter-selection of LMP1/CD30-expressing GC B cells (supplemental Figure 9C). These results suggest that LMP1/CD30-expression in pre-GC B cells interferes with the GC reaction.

LMP1/CD30-expression drives PC-differentiation in GC and non-GC B cells

To restrict LMP1/CD30-expression to GC (and post-GC) B cells, thereby preventing the blockade of GC establishment by LMP1/CD30, we crossed $LMP1/CD30^{flSTOP}$ mice with Cγ1-Cre mice (hereafter named LMP1/CD30//γ1-Cre), resulting in the deletion of the stop-cassette in GC B cells[25]. For controls, we used the reporter-mice $R26/CAG\text{-}CAR\Delta1^{StopF}$, expressing a truncated version of the human coxsackie/adenovirus-receptor (CAR) upon Cre-mediated recombination[26]. Immunization with NP-CGG resulted in significant more $reporter^+$ B cells in LMP1/CD30//γ1-Cre-mice than in controls 5d and 14d post immunization (p.i.) (supplemental Figure 10A). Since the percentage of GC B cells within the $reporter^+$ cells was lower in LMP1/CD30//γ1-Cre-mice (supplemental Figure 10B), the increased number of $reporter^+$ cells could be mainly attributed to non-GC B cells (Figure 6A). Within the $reporter^+$ GC cells the percentage of hapten-binding (NP^+) B

cells was lower in LMP1/CD30//γ1-Cre-mice than in controls (supplemental Figure 10C). However, total percentages of reporter$^+$ GC and NP$^+$ GC B cells within all lymphocytes were comparable in LMP1/CD30//γ1-Cre- and CAR//γ1-Cre-mice (Figure 6A). In addition, GCs were clearly visible in splenic sections of LMP1/CD30//γ1-Cre mice 14d p.i. (Figure 6B). These data indicate that GC B cells are generated after TD-immunization of LMP1/CD30//γ1-Cre mice.

Further characterization of reporter$^+$ lymphocytes revealed higher percentages of B220^{low}CD138$^+$ and CD23^{low}CD43$^+$ cells in LMP1/CD30//γ1-Cre-mice in comparison to controls 5d and 14d p.i. (Figure 6C, supplemental Figure 11A). Fourteen days p.i. the increased CD23^{low}CD43$^+$ cell population could be attributed to the non-GC compartment, whereas B220^{low}CD138^{high} cells were elevated both in the GC as well as non-GC B cell fractions (Supplemental Figure 11B). All B220^{low}CD138^{high} cells were CD23^{low}CD43$^+$ and expressed low levels of CD19 in accord with a PB/PC phenotype (Supplemental Figure 11C). A certain fraction of CD23^{low}CD43$^+$ cells was still CD19$^+$, and therefore are most likely LMP1/CD30-expressing B1 cells (Supplemental Figure 11C). Furthermore, the percentages of reporter$^+$ IgG1$^+$ cells were lower in LMP1/CD30//γ1-Cre-mice compared with controls (Supplemental Figure 11D). Moreover IgG1 levels were lower on the surface of B cells from LMP1/CD30//γ1-Cre mice suggesting that the cells already start to differentiate to PC[35]. Taken together, these data showed that TD-immunization of LMP1/CD30//γ1-Cre-mice results in similar percentages of reporter$^+$ GC B cells as in controls, but leads to more reporter$^+$ cells with a non-GC phenotype such as B1 cells and PBs. NP-specific IgM PC numbers were higher in the spleens of LMP1/CD30//γ1-Cre-mice but NP-IgG1 PC numbers were comparable between genotypes. Serum NP-specific IgM and total NP-IgG1 titers were increased in mutants compared with controls whereas high affinity NP-IgG1 antibodies were comparable between both genotypes (Figure 6D). These data suggest that LMP1/CD30-expression enhances the production of NP-specific IgM- and low-affinity, short-lived IgG1-PC, which may no longer be detected in ELISpot-analyses 14d p.i.. Nevertheless, they can contribute to the increased titers of NP-specific IgG1-antibodies in the serum. Since we observed the strong and fast upregulation of IRF4 upon CD40-stimulation *in vitro,* we tested whether LMP1/CD30-expression enhances PC-differentiation through upregulation of

IRF4. LMP1/CD30-expression did not lead to higher IRF4-expression in all reporter$^+$ lymphocytes, but to a higher percentage of IRF4$^+$ cells 5d and 14d p.i (Supplemental Figure 12A). At day 5, IRF4$^+$ B cells were localized mainly at the T/B cell border suggesting that they originate from early GC as described by Zhang et al[36] or from LMP1/CD30-expressing B1 cells (Figure 6E). At day 14 p.i. IRF4$^+$ B cells were mainly localized at the edge of GCs or follicles, assuming that these cells are going to exit the GC reaction (Figure 6E). Interestingly, the percentage of IRF4$^+$ cells was higher in the fractions of both centroblasts (CB) and centrocytes (CC) of LMP1/CD30//γ1-Cre-mice (Figure 6F, supplemental Figure 12B), indicating that CD30-signaling in GC B cells contributes to the generation and/or expansion of IRF4$^+$ B cells in the dark and light zone (DZ and LZ) of the GC.

Lymphomas with a B1-like phenotype arise in the spleen and PerC of LMP1/CD30-mice

Our results suggest that upon antigenic stimulation, chronic CD30-signaling results in enhanced production of B1 cells and PBs, which display an enhanced proliferation as indicated by increased Ki-67 levels (supplemental Figure 13A). To test whether the expansion of B1 cells and PB cells leads to lymphoma development, we aged cohorts of mice. LMP1/CD30-mice were analyzed together with age-matched controls when they showed signs of morbidity (supplemental Figure 13B). Compared with young LMP1/CD30- and old control-mice, diseased aged LMP1/CD30-mice had an increased splenomegaly with elevated B- and T-cell numbers (Figure 7A). A high percentage of B cells displayed the phenotype B220^{low}CD21^{low}CD23^{low}CD43$^+$ and were either CD5$^+$ or CD5$^-$ (Figure 7B and supplemental Figure 13C) in accord with a B1a- or B1b-phenotype. Most B cells were CD138$^-$ but expressed higher levels of IRF4 compared with age-matched control B cells (Figure 7C, supplemental Figure 13D). T cells were highly activated and shifted to an effector memory T-cell phenotype (Figure 7D). In addition, B1a and B1b cells were strongly expanded in the PerC (Figure 7E, supplemental Figure 13E) and the B220^{low}CD21^{low}CD23^{low} population was strongly enriched in the blood (Figure 7F). Histopathological examination of the spleen revealed a disrupted structure, nodular infiltration of the white pulp by lymphocytes and many intermingled blasts as well as a diffuse

infiltration of the red pulp. (Figure 7G). Other samples showed confluent sheets of blasts. Around 80% of mice developed monoclonal lymphomas (Figure 7H, Supplemental Table 2).
These data indicated that chronic CD30-signaling in B cells leads to lymphoma development in aged mice.

Discussion

Currently, the contribution of CD30-signaling to lymphoma development or its function in B cell physiology is poorly understood. Studies in normal B cells were hampered by the very low numbers of $CD30^+$ B cells *in vivo*. Studies of CD30-deficient mice did not reveal a clear phenotype, probably because of the redundancy of TNF-R-signaling *in vivo*. We chose an alternative approach by studying the effect of constitutively active CD30-signaling in B cells. Here we provide evidence that chronic CD30-signaling triggers the expansion of B1 cells and PBs resulting in B-cell lymphoma development in aged mice.

B1 cell and PC expansion in young LMP1/CD30-mice correlated well with expression data showing the upregulation of CD30 in B1 cells and PC-progenitors[37]. Some activated $CD4^+CD44^+$ T cells in the spleen and the PerC express the CD30L[38] and might stimulate B1 cells resulting in their proliferation and PC-differentiation. B1 cells produce natural antibodies of the IgM and IgG3-subtype and are the major source of IgA antibodies[39,40]. Moreover, B1 and MZB cells mainly generate IgM and IgG3 antibodies during TI-2 immune responses[41,42]. Thus, the elevated total antibody-titers in LMP1/CD30-mice may be due to higher titers of natural antibodies and IgA antibodies produced by LMP1/CD30-expressing B1 cells as well as to enhanced TI-immune responses. Our data suggest that the increased B-cell population in LMP1/CD30-mice consists of a mixture of splenic B1 cells and (pre-)PB that have a very similar phenotype. Our assumption is supported by previous publications showing that splenic B1 cells contain a fraction of antibody-secreting cells even in non-stimulated control-mice[43], and that human B1 cells resemble pre-PBs in some aspects[44]. In CD40-stimulated B cells, CD30-signaling might enhance PC-differentiation by increasing STAT6- and STAT3-phosphorylation as well as NF-κB activation. This might result in enhanced upregulation of IRF4 and BLIMP-1 and thus

contribute to PB differentiation. Previous reports demonstrated that pSTAT3 resulted in the upregulated expression of BLIMP1 and was necessary for differentiation of GC B cells to PCs[32,33,45].

We suggest that co-stimulation of the B cell receptor (BCR) and CD40, as it occurs in extrafollicular B cells as well as during positive selection of CC, leads to the upregulation of CD30. Our data suggest that $CD30^+$ B cells might be prone to enter PC-differentiation. Physiologically, PC-differentiation seems to be initiated in some CC, but small percentages of BLIMP-1^+ and $IRF4^+$ B cells are also present within CB[35]. In LMP1/CD30//γ1-Cre -mice the percentage of $IRF4^+$ B cells was clearly increased in both CB and CC. Recently, Weniger and colleagues provided evidence that $CD30^+$ GC B cells represent positively selected CC, which return to the DZ to undergo further rounds of proliferation and hypermutation[46]. Accordingly, $IRF4^+$ cells in LMP1/CD30-mice might arise in the LZ, when CC receive a CD40 signal from T cells in the process of positive selection. Like $CD30^+$ B cells they may migrate back to the DZ. During their return to the DZ most of the $CD30^+$ B cells might switch off the CD30-signal because they lose their interaction with activated T cells. In contrast, CD30-signaling remains constitutively active in LMP1/CD30-expressing GC B cells in the DZ and might therefore – due to the high IRF4 levels – result in premature differentiation to IgM and low affinity IgG1 PC. Interestingly, Weniger and colleagues found that STAT3 and STAT6 gene sets were significantly enriched in extrafollicular $CD30^+$ B cells, assuming that these cells are triggered by CD30L-expressing cells[46]. $CD30^+$ extrafollicular B cells are highly activated and proliferative[46], suggesting that they undergo several rounds of division before they enter PC-differentiation. PBs can persist for months[47]. Consequently, LMP1/CD30-mice might contain a larger pool of long-lived PBs that continuously differentiates to PCs. These (pre-)PB might be permanently triggered by persistent antigens and therefore continuously re-enter the cell cycle. This might be a potential risk for lymphoma development. Indeed, aged LMP1/CD30-mice developed B-cell lymphomas with a B1b- or B1a-phenotype and elevated levels of IRF4. The lymphoma cells were mostly present in the spleen and PerC and replaced all other B-cell populations. Interestingly, PELs, which are also $CD30^+$, do not have a solid tumor mass but cause serious effusions in body cavities such as the pleural and peritoneal cavities. Thus, the marked expansion of B1 cells in

LMP1/CD30-mice resembles PELs in some aspects, although they do not show an IgM^- phenotype. Interestingly, soluble CD30 levels were associated with an increased risk of developing NHL[21-23], suggesting that continuous CD30-signaling might drive lymphoma development. Therefore, our mouse model might mimic chronic CD30-signaling induced by continuous immune-stimulation such as chronic viral infections or autoimmune diseases. We provide experimental proof that chronic CD30-signaling results in lymphoma development. However, our data also indicate that chronic CD30-signaling alone is not sufficient to induce lymphomagenesis. Indeed, all described tumors mainly consisted of a monoclonal cell population, indicating that they derived from single secondary mutation events. It will be interesting to determine which mutations cooperate with chronic CD30-signaling to drive lymphomagenesis.

Acknowledgement

This work was supported by the Deutsche Krebshilfe (111426), the Deutsche Forschungsgemeinschaft (DFG ZI1382/4-1 and SFB1243) and the Jose Carreras Stiftung (DJCLS R 13/02). We thank the animal facility of the Helmholtz Center and our animal care takers, headed by Michael Hagemann, for excellent housing of the mice. This work benefitted from data assembled by the ImmGen consortium. We thank Dr. Podack for kindly providing the vector pBmgNeo CD30-5.2 which contained the full length CD30 cDNA clone and Ralf Küppers for helpful discussions and comments on the manuscript.

Authorship contributions

SP, PF, AP, ML, SE performed experiments, LK, A-IS, AF performed and evaluated histology, RK generated LMP1/$CD30^{stopfl}$ mice, LJS performed in silico analysis, LJS and UZS designed experiments, SP, PF, LJS and UZS prepared and wrote the manuscript.

Disclosure of Conflict of Interest

The authors have no conflict of interest to declare.

References

1. Younes A, Aggarwall BB. Clinical implications of the tumor necrosis factor family in benign and malignant hematologic disorders. *Cancer.* 2003;98(3):458-467.
2. Schwab U, Stein H, Gerdes J, et al. Production of a monoclonal antibody specific for Hodgkin and Sternberg-Reed cells of Hodgkin's disease and a subset of normal lymphoid cells. *Nature.* 1982;299(5878):65-67.
3. Stein H, Foss HD, Durkop H, et al. CD30(+) anaplastic large cell lymphoma: a review of its histopathologic, genetic, and clinical features. *Blood.* 2000;96(12):3681-3695.
4. Klein U, Gloghini A, Gaidano G, et al. Gene expression profile analysis of AIDS-related primary effusion lymphoma (PEL) suggests a plasmablastic derivation and identifies PEL-specific transcripts. *Blood.* 2003;101(10):4115-4121.
5. Bhatt S, Ashlock BM, Natkunam Y, et al. CD30 targeting with brentuximab vedotin: a novel therapeutic approach to primary effusion lymphoma. *Blood.* 2013;122(7):1233-1242.
6. Hu S, Xu-Monette ZY, Balasubramanyam A, et al. CD30 expression defines a novel subgroup of diffuse large B-cell lymphoma with favorable prognosis and distinct gene expression signature: a report from the International DLBCL Rituximab-CHOP Consortium Program Study. *Blood.* 2013;121(14):2715-2724.
7. Slack GW, Steidl C, Sehn LH, Gascoyne RD. CD30 expression in de novo diffuse large B-cell lymphoma: a population-based study from British Columbia. *Br J Haematol.* 2014;167(5):608-617.
8. Kadin ME. Regulation of CD30 antigen expression and its potential significance for human disease. *Am J Pathol.* 2000;156(5):1479-1484.
9. Hansen HP, Dietrich S, Kisseleva T, et al. CD30 shedding from Karpas 299 lymphoma cells is mediated by TNF-alpha-converting enzyme. *J Immunol.* 2000;165(12):6703-6709.
10. Durkop H, Latza U, Hummel M, Eitelbach F, Seed B, Stein H. Molecular cloning and expression of a new member of the nerve growth factor receptor family that is characteristic for Hodgkin's disease. *Cell.* 1992;68(3):421-427.
11. Bowen MA, Lee RK, Miragliotta G, Nam SY, Podack ER. Structure and expression of murine CD30 and its role in cytokine production. *J Immunol.* 1996;156(2):442-449.
12. Goldie-Cregan LC, Croager EJ, Abraham LJ. Characterization of the murine CD30 ligand (CD153) gene: gene structure and expression. *Tissue Antigens.* 2002;60(2):139-146.
13. Croager EJ, Abraham LJ. Characterisation of the human CD30 ligand gene structure. *Biochim Biophys Acta.* 1997;1353(3):231-235.
14. Cerutti A, Schaffer A, Shah S, et al. CD30 is a CD40-inducible molecule that negatively regulates CD40-mediated immunoglobulin class switching in non-antigen-selected human B cells. *Immunity.* 1998;9(2):247-256.
15. Shanebeck KD, Maliszewski CR, Kennedy MK, et al. Regulation of murine B cell growth and differentiation by CD30 ligand. *Eur J Immunol.* 1995;25(8):2147-2153.
16. Amakawa R, Hakem A, Kundig TM, et al. Impaired negative selection of T cells in Hodgkin's disease antigen CD30-deficient mice. *Cell.* 1996;84(4):551-562.

17. Gaspal FMC, Kim MY, McConnell FM, Raykundalia C, Bekiaris V, Lane PJL. Mice Deficient in OX40 and CD30 Signals Lack Memory Antibody Responses because of Deficient CD4 T Cell Memory. *The Journal of Immunology.* 2005;174(7):3891-3896.
18. Carbone A, Cesarman E, Spina M, Gloghini A, Schulz TF. HIV-associated lymphomas and gamma-herpesviruses. *Blood.* 2009;113(6):1213-1224.
19. Purdue MP, Lan Q, Martinez-Maza O, et al. A prospective study of serum soluble CD30 concentration and risk of non-Hodgkin lymphoma. *Blood.* 2009;114(13):2730-2732.
20. Vermeulen R, Hosnijeh FS, Portengen L, et al. Circulating soluble CD30 and future risk of lymphoma; evidence from two prospective studies in the general population. *Cancer Epidemiol Biomarkers Prev.* 2011;20(9):1925-1927.
21. Purdue MP, Lan Q, Kemp TJ, et al. Elevated serum sCD23 and sCD30 up to two decades prior to diagnosis associated with increased risk of non-Hodgkin lymphoma. *Leukemia.* 2015;29(6):1429-1431.
22. De Roos AJ, Mirick DK, Edlefsen KL, et al. Markers of B-cell activation in relation to risk of non-Hodgkin lymphoma. *Cancer Res.* 2012;72(18):4733-4743.
23. Hosnijeh FS, Portengen L, Spath F, et al. Soluble B-cell activation marker of sCD27 and sCD30 and future risk of B-cell lymphomas: A nested case-control study and meta-analyses. *Int J Cancer.* 2016;138(10):2357-2367.
24. Willis SN, Good-Jacobson KL, Curtis J, et al. Transcription factor IRF4 regulates germinal center cell formation through a B cell-intrinsic mechanism. *J Immunol.* 2014;192(7):3200-3206.
25. Casola S, Cattoretti G, Uyttersprot N, et al. Tracking germinal center B cells expressing germ-line immunoglobulin gamma1 transcripts by conditional gene targeting. *Proc Natl Acad Sci U S A.* 2006;103(19):7396-7401.
26. Heger K, Kober M, Riess D, et al. A novel Cre recombinase reporter mouse strain facilitates selective and efficient infection of primary immune cells with adenoviral vectors. *Eur J Immunol.* 2015;45(6):1614-1620.
27. Homig-Holzel C, Hojer C, Rastelli J, et al. Constitutive CD40 signaling in B cells selectively activates the noncanonical NF-kappaB pathway and promotes lymphomagenesis. *J Exp Med.* 2008;205(6):1317-1329.
28. Cattoretti G, Shaknovich R, Smith PM, Jack HM, Murty VV, Alobeid B. Stages of Germinal Center Transit Are Defined by B Cell Transcription Factor Coexpression and Relative Abundance. *The Journal of Immunology.* 2006;177(10):6930-6939.
29. Hojer C, Frankenberger S, Strobl LJ, et al. B-cell expansion and lymphomagenesis induced by chronic CD40 signaling is strictly dependent on CD19. *Cancer Res.* 2014;74(16):4318-4328.
30. Oracki SA, Walker JA, Hibbs ML, Corcoran LM, Tarlinton DM. Plasma cell development and survival. *Immunol Rev.* 2010;237(1):140-159.
31. Minnich M, Tagoh H, Bonelt P, et al. Multifunctional role of the transcription factor Blimp-1 in coordinating plasma cell differentiation. *Nat Immunol.* 2016;17(3):331-343.
32. Reljic R, Wagner SD, Peakman LJ, Fearon DT. Suppression of signal transducer and activator of transcription 3-dependent B lymphocyte terminal differentiation by BCL-6. *J Exp Med.* 2000;192(12):1841-1848.
33. Diehl SA, Schmidlin H, Nagasawa M, et al. STAT3-Mediated Up-Regulation of BLIMP1 Is Coordinated with BCL6 Down-Regulation to Control Human Plasma Cell Differentiation. *The Journal of Immunology.* 2008;180(7):4805-4815.
34. Grumont RJ, Gerondakis S. Rel induces interferon regulatory factor 4 (IRF-4) expression in lymphocytes: modulation of interferon-regulated gene expression by rel/nuclear factor kappaB. *J Exp Med.* 2000;191(8):1281-1292.

35. Krautler NJ, Suan D, Butt D, et al. Differentiation of germinal center B cells into plasma cells is initiated by high-affinity antigen and completed by Tfh cells. *J Exp Med.* 2017;214(5):1259-1267.
36. Zhang Y, Tech L, George LA, et al. Plasma cell output from germinal centers is regulated by signals from Tfh and stromal cells. *J Exp Med.* 2018;215(4):1227-1243.
37. Jourdan M, Caraux A, Caron G, et al. Characterization of a transitional preplasmablast population in the process of human B cell to plasma cell differentiation. *J Immunol.* 2011;187(8):3931-3941.
38. Tang C, Yamada H, Shibata K, et al. A novel role of CD30L/CD30 signaling by T-T cell interaction in Th1 response against mycobacterial infection. *J Immunol.* 2008;181(9):6316-6327.
39. Savage HP, Yenson VM, Sawhney SS, Mousseau BJ, Lund FE, Baumgarth N. Blimp-1-dependent and -independent natural antibody production by B-1 and B-1-derived plasma cells. *J Exp Med.* 2017;214(9):2777-2794.
40. Meyer-Bahlburg A. B-1 cells as a source of IgA. *Ann N Y Acad Sci.* 2015;1362:122-131.
41. Snapper CM, McIntyre TM, Mandler R, et al. Induction of IgG3 secretion by interferon gamma: a model for T cell-independent class switching in response to T cell-independent type 2 antigens. *J Exp Med.* 1992;175(5):1367-1371.
42. Martin F, Kearney JF. Marginal-zone B cells. *Nat Rev Immunol.* 2002;2(5):323-335.
43. Yang Y, Tung JW, Ghosn EE, Herzenberg LA, Herzenberg LA. Division and differentiation of natural antibody-producing cells in mouse spleen. *Proc Natl Acad Sci U S A.* 2007;104(11):4542-4546.
44. Covens K, Verbinnen B, Geukens N, et al. Characterization of proposed human B-1 cells reveals pre-plasmablast phenotype. *Blood.* 2013;121(26):5176-5183.
45. Fornek JL, Tygrett LT, Waldschmidt TJ, Poli V, Rickert RC, Kansas GS. Critical role for Stat3 in T-dependent terminal differentiation of IgG B cells. *Blood.* 2006;107(3):1085-1091.
46. Weniger MA, Tiacci E, Schneider S, et al. Human CD30+ B cells represent a unique subset related to Hodgkin lymphoma cells. *J Clin Invest.* 2018;128(7):2996-3007.
47. Hsu MC, Toellner KM, Vinuesa CG, Maclennan IC. B cell clones that sustain long-term plasmablast growth in T-independent extrafollicular antibody responses. *Proc Natl Acad Sci U S A.* 2006;103(15):5905-5910.
48. Shi W, Liao Y, Willis SN, et al. Transcriptional profiling of mouse B cell terminal differentiation defines a signature for antibody-secreting plasma cells. *Nat Immunol.* 2015;16(6):663-673.

Figures Legends

Figure 1. Expression of CD30 on B cells. (A) The histogram shows an overlay of the CD30 surface expression on B1a ($CD5^{+}B220^{low}CD19^{+}$), B1b ($CD5^{low}B220^{low}CD19^{+}$) and B2 ($B220^{high}CD19^{+}$) cells of the PerC and the spleen. n=3 (B) *In silico* analysis of immgen.org data showing the CD30 (TNFRSF8) mRNA expression in different B-cell populations of the PerC and the spleen. (C) The overlay shows CD30 and CD86 surface expression of splenic B cells in the absence of stimulation (day 0) and after 1 or 3 days of CD40+IgM-stimulation. Staining of CD86 was used as positive control for B-cell activation. n=3 (D) CD30 mRNA expression

(FPKM: fragments per kilobase of exon per million reads mapped) at different B-cell activation stages after CD40- and LPS-stimulation of FoB cells: FoB: unstimulated FoB cells; CD40/IL4-blasts ($B220^{+}CD138^{-}$), CD40/IL4/IL5 PB ($B220^{+}CD138^{-}$); LPS blasts ($BLIMP1^{-}CD138^{-}$), LPS PB SDC1^{-} ($BLIMP1^{+}CD138^{-}$), LPS PB SDC1^{+} ($BLIMP1^{+}CD138^{+}$) and splenic PCs (SDC1=Syndecan1=CD138). CD30 mRNA expression was determined by *in silico* analysis of expression data published by Shi and coworkers[48]. (E) The histogram shows an overlay of CD30 surface expression of IRF4^{+} versus IRF4^{-} splenic B cells. Gating was performed as shown in the dot plot. Dot plots were pre-gated on a large lymphocyte gate and Thy1.2^{-} cells. The analysis is representative of 2 independent experiments with 3 mice each.

Figure 2. Constitutive CD30 expression in B cells leads to the expansion of B1 cells in the spleen and PerC. (A) Splenic weights and absolute splenic B- and T-cell numbers from LMP1/CD30-mice and controls (ctrl) with 8-12 weeks of age are shown. (B) Splenic sections from LMP1/CD30- and control-mice were stained for IgM (brown/red), CD3 (light blue) and MOMA-1 (dark blue) to visualize B cells, T cells and metallophilic macrophages, respectively. Slides were analyzed with an Axioskop (Zeiss) with a Zeiss Plan NEOFLUAR objective 10x/0.3. Images were obtained with an AxioCam MRc5 digital camera in combination with AxioVision rel.4.6.3.0 software (Carl Zeiss MicroImaging GmbH, Jena, Germany). (C) Splenic B lymphocytes ($CD19^{+}$) were analyzed for the expression of IgM/IgD, the distribution of FoB cells ($CD21^{int}CD23^{+}$) and MZ B cells ($CD21^{high}CD23^{low}$), for B1 ($CD43^{+}CD23^{low}$) and B2 ($CD43^{-}CD23^{+}$) cells as well as for B1a ($CD5^{+}B220^{low}$), B1b ($CD5^{low}B220^{low}$), and B2 ($B220^{+}CD5^{low}$) by flow cytometry. n≥6 (D) Total numbers of B lymphocytes ($CD19^{+}$) in the PerC were counted and calculated based on their staining, B1a ($CD5^{+}B220^{low}$), B1b ($CD5^{low}B220^{low}$) and B2 ($CD5^{low}B220^{+}$). B cells from LMP1/CD30-mice were gated on hCD2. Data were collected from 8–16 weeks old mice. Numbers in the FACS plots indicate the mean and standard deviation (SD) values of the percentages of the gated B cell populations.

Figure 3. Constitutive CD30 expression expands PCs *in vivo* and *in vitro*. (A) Flow cytometric analysis of splenic and BM lymphocytes stained for PCs ($B220^{-/low}CD138^{+}$). Cells were pre-gated using a large lymphocyte gate. n≥6. Numbers in the FACS plots indicate the mean and SD values of the percentages of the gated populations. (B) Serum concentration of total immunoglobulins of the indicated isotypes were determined by ELISA. Horizontal bars represent the mean value. (C) qRT-PCR analysis showing the relative expression of Prdm1 (BLIMP1), Xbp1 and Pax5 in $CD43^{+}CD23^{low}$ B1 versus $CD43^{-}CD23^{+}$ B2 cells from control and LMP1/CD30-mice. Expression was standardized to the house keeping gene Ywhaz. (D) Relative mean fluorescence intensity (MFI) of IRF4 in B1 ($CD43^{+}CD23^{low}$) and B2 cells ($CD43^{-}CD23^{+}$) from LMP1/CD30 and control-mice. Relative MFIs were related to the MFI of control B2 cells, which was set as 1. Data are from three independent experiments (E) B1 ($CD43^{+}CD23^{low}$) and B2 cells ($CD43^{-}CD23^{+}$) were analyzed for their CD138/B220 expression and shown as an overlay. n≥4. (F) $CD138^{-}$ B1 cells ($CD43^{+}CD23^{low}$) were sorted and reanalyzed as described in Supplemental Figure 6. After sorting, B1 cells ($CD138^{-}CD43^{+}CD23^{low}$) were cultivated without stimulation for 3d and subsequently analyzed for their CD138/B220 expression. The dot plot shows the gating strategy and the graph compiles the data of the percentages of $CD138^{high}B220^{low}$ cells from the indicated genotypes from three independent experiments.

Figure 4. Increased PC-differentiation of B2 cells upon CD40-stimulation (A, B) Sorted splenic B2 cells ($CD23^{+}CD43^{-}$) from LMP1/CD30- and control-mice were stimulated with anti-CD40-antibody for 3d and analyzed for their B220/CD138 and CD43/CD23 surface expression. The sorting strategy and the purity of the sorted B2 cells are shown in supplemental Figure 7A. The numbers in the FACS plots indicate mean and SD values of the percentages of the gated populations in the different FACS analyses. (C) $CD43^{+}CD23^{low}$ and $CD43^{-}CD23^{+}$ cells were gated as shown in (B). The B220/CD138 staining of $CD43^{+}CD23^{low}$ and $CD43^{-}CD23^{+}$ cells is shown as overlay. n≥3. D) The histograms show overlays of the CXCR4 and CD22 surface expression of $CD43^{+}CD23^{low}$ and $CD43^{-}CD23^{+}$ from control and LMP1/CD30 mice. (E) Determination of pSTAT6 and pSTAT3 levels in nuclear extracts of splenic B cells stimulated with an anti-CD40-antibody for the indicated time points. Splenic B cells

were purified by MACS using magnetic beads binding to CD43 to remove most of the B1 cells. The protein levels were analyzed and quantified using the WES separation system and software. Determination of p65 (F) and IRF4 (G) in cytoplasmic and nuclear extracts from the indicated genotypes. B cells purified by CD43 depletion were stimulated for 10 min with anti-CD40-antibody. The protein levels of p65 and IRF4 were analyzed and quantified using the WES separation system and software. For each mouse, the value after stimulation was standardized with the corresponding unstimulated value n≥5.

Figure 5. CD30-signaling enhances the expansion of B1a cells and PCs upon TI-2- immunization. (A) Mice were immunized with NP-Ficoll and analyzed after 14 days p.i. Percentages of PCs ($CD138^{+}B220^{low}Gr1^{-}Thy1.2.^{-}CD11b^{-}$) and B1a cells ($CD5^{+}CD19^{+}B220^{low}$) in the spleen were determined by flow cytometry. 14 days after immunization IgM- and IgG3-secreting PCs from the spleen were determined by ELISpot-analysis (B) and serum titers of IgM- and IgG3-antibodies binding to NP17-BSA (C) by ELISA. (D) Splenic sections from LMP1/CD30 and ctrl mice were stained for GC B cells (PNA, blue), Metallic macrophages surrounding the primary follicles (Moma, blue), and B cells (IgM, red/brown) 14 days after NP-CGG immunization.

Figure 6. CD30-signaling enhances PC-differentiation upon TD-immunization with NP-CGG. (A) Displayed are the percentages of $reporter^{+}$ lymphocytes, of $CD38^{low}CD95^{high}$ $reporter^{+}$ GC B cells and NP^{+} $reporter^{+}$ GC B cells in LMP1/CD30//γ1-Cre mice and CAR//γ1-Cre upon NP-CGG immunization at the indicated time points. The gating strategy of $reporter^{+}$ lymphocytes, GC B cells and NP^{+} GC B cells as well as graphs compiling values of different experiments including the statistics are shown in supplemental Figure 10 A-C. (B) GCs were clearly visible 14d after immunization with NP-CGG in LMP1/CD30//γ1-Cre and CAR//γ1-Cre mice. Splenic sections from these mice as well as from unimmunized control (ctrl) mice were stained for GC B cells (PNA, blue) and IgM^{+} cells (IgM, brown). Slices were analysed as described in Figure 2B (C) The left graph shows the percentages of $CD43^{+}CD23^{low}$ cells within the fraction of $reporter^{+}$ (CAR^{+}, $hCD2^{+}$) lymphocytes after 5d and 14d p.i. in LMP1/CD30//γ1-Cre ($hCD2^{+}$) and CAR//γ1-Cre (CAR^{+}) mice. The right graph shows the percentages of $CD138^{+}B220^{low}$ PBs and PCs in the fraction of reporter positive (CAR^{+}, $hCD2^{+}$) lymphocytes. The corresponding gating strategies

are shown in Supplemental Figure 11A. (D) Upper row: NP-IgM as well as total (NP13) and high affinity (NP4) NP-specific IgG1 secreting PCs were determined by ELISpot analysis 14d p.i. using splenocytes from the two genotypes. Lower row: Serum titers of the indicated antibodies were measured by ELISA 14d after immunization with NP-CGG. (E) Splenic sections from LMP1/CD30//γ1-Cre, CAR//γ1-Cre 5d and 14d after immunization with NP-CGG and unimmunized (n.i.) ctrl mice were stained for GC B cells (GL7, green), B cells (B220, red) and PBs (IRF4, cyan). The images of immunofluorescences were obtained with the Leica TCS SP5 II with an 8 kHz resonant scanner and a HCX PL APO CS 20x objective and the LAS AF software. (F) The percentage of $IRF4^{+}$ cells in the fraction of $reporter^{+}$ centroblasts (CB) ($CXCR4^{high}CD86^{low}$) and centrocytes (CC) ($CXCR4^{low}CD86^{high}$) was determined 14d p.i.. The graph compiles the percentages of $IRF4^{+}$ cells in CBs and CCs from different experiments. The gating strategy of $reporter^{+}$ CB and CC as well as $IRF4^{+}$ cells is shown in Supplemental Figure 12B.

Figure 7. Lymphomas with a B1-like phenotype arise in the spleen and PerC of aged LMP1/CD30-mice. (A) Splenic weights, B- and T-cell numbers in the spleen of aged LMP1/CD30-mice compared with old control-mice and young LMP1/CD30-mice. (B) Representative flow cytometric analyses of splenic B cells ($CD19^{+}$) for CD43/CD23 and CD21/CD23 surface expression. The graph compiles the percentages of the $CD21^{low}CD23^{low}$ population of aged mice. C) Flow cytometric analysis of splenic B cells to determine the percentage of PCs ($B220^{low}CD138^{+}$). Numbers represent means and SDs. (D) T cells in the spleen of aged mice were analyzed to determine the percentages and SD of naïve T cells ($CD62L^{high}CD44^{low}$), central memory T cells ($CD62L^{high}CD44^{high}$) and effector memory T cells ($CD62^{low}CD44^{+}$). (E) Diagram showing total B-cell numbers in the PerC. (F) Flow cytometric analysis of the $CD21^{low}CD23^{low}$ population in blood B lymphocytes ($CD19^{+}$). Numbers in the FACS plots indicate the mean and SD values of the percentages of the gated populations. (G) H&E staining as well as anti-B220- (B cells) and anti-CD3- (T cells) immunohistochemistry of spleen sections of an aged control and LMP1/CD30 mouse. Sections were scanned with an AxioScan.Z1 digital slide scanner (Zeiss, Jena, Germany) equipped with a 20x magnification objective (EC Plan-Neofluar 20x/0.50, Zeiss, Jena, Germany) and a Hitachi HV-F202SCL

3CCD Camera. Imaging acquisition was performed using an Imaging Software ZEN 2.3 SP1 blue edition (Zeiss, Jena, Germany) and NetScope Viewer Pro (Net-Base Software GmbH, Freiburg, Germany). (H) Kaplan-Meier curve of lymphoma development in LMP1/CD30-mice. Significance of lymphoma development was calculated by the log-rank (Mantel-Cox) test.

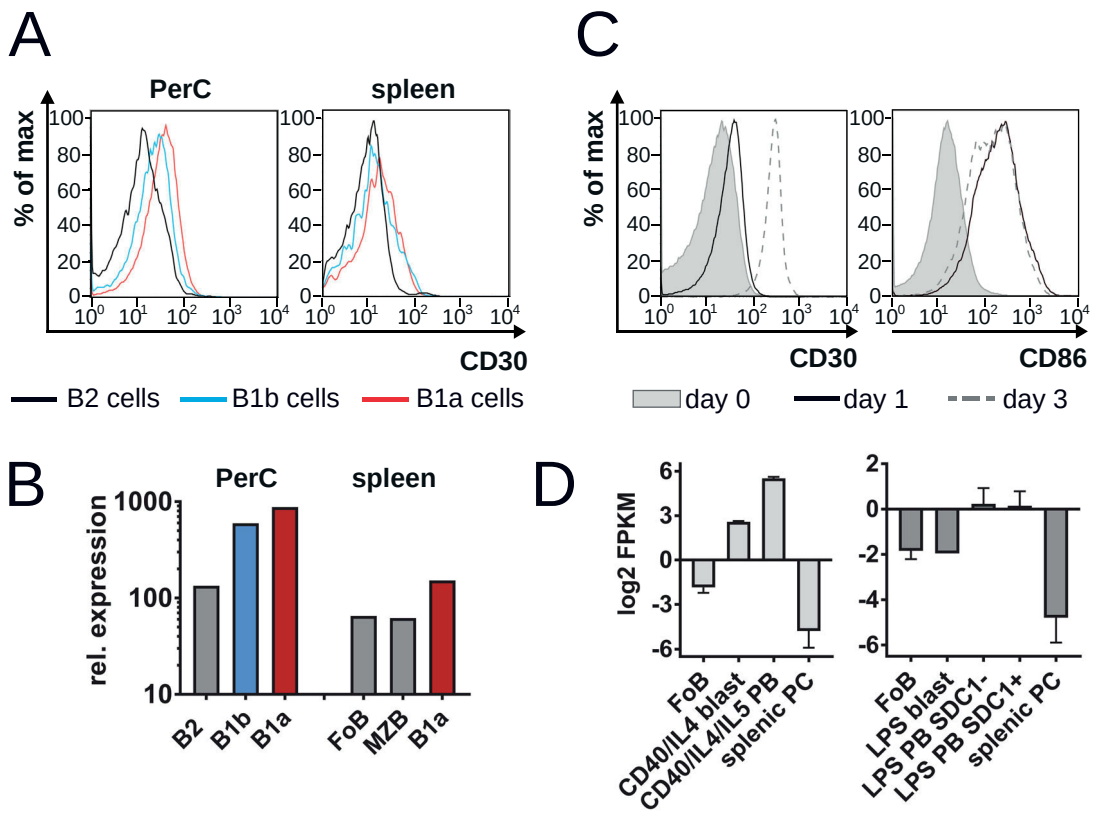
A
PerC
spleen
% of max
CD30
B2 cells
B1b cells
B1a cells
C
CD30
CD86
day 0
day 1
day 3
B
rel. expression
B2
B1b
B1a
FoB
MZB
D
log2 FPKM
FoB
CD40/IL4 blast
CD40/IL4/IL5 PB
splenic PC
LPS blast
LPS PB SDC1-
LPS PB SDC1+
E
IRF4
CD19
IRF4-
IRF4+
CD30

Figure 1

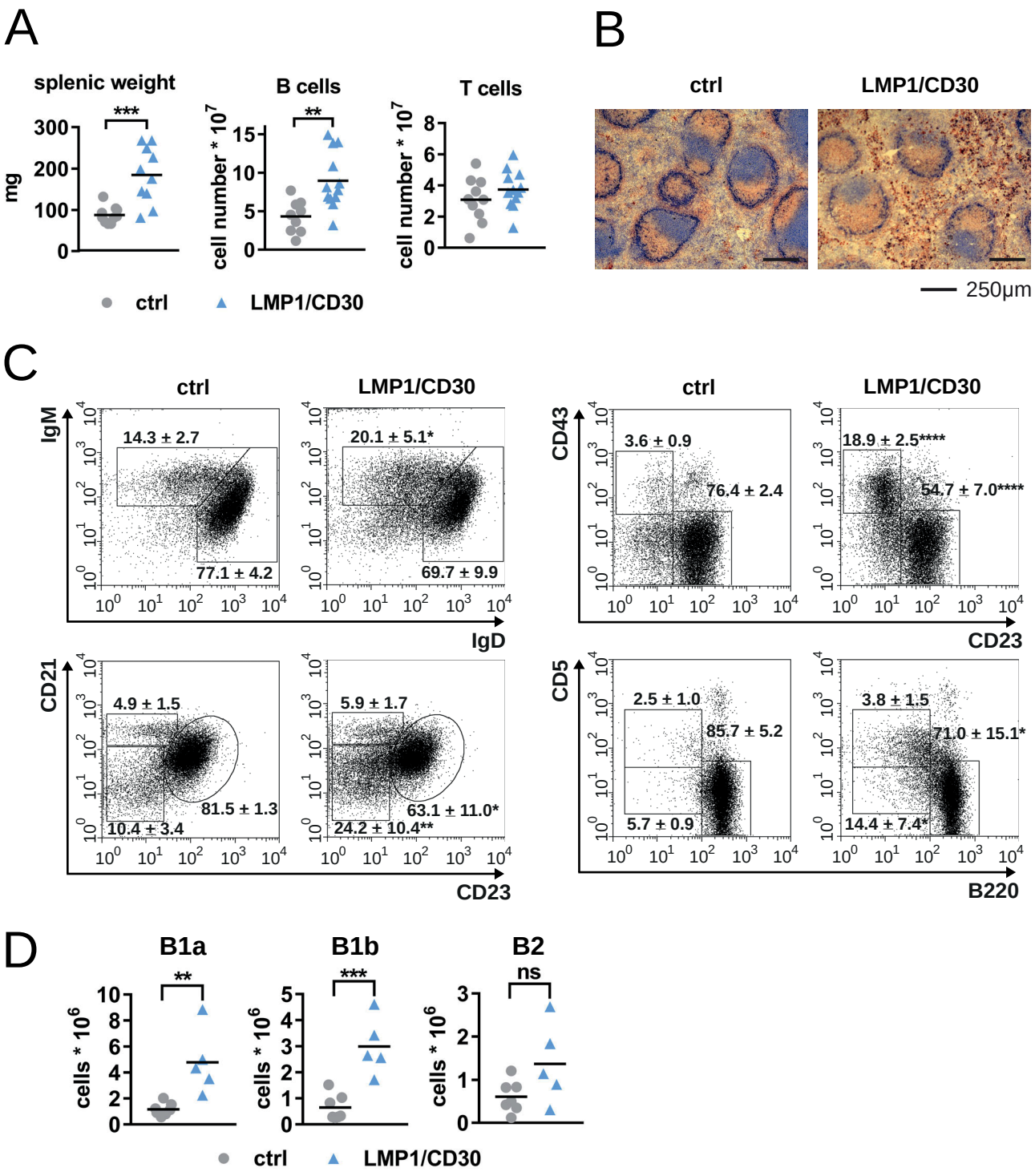
A
splenic weight
mg
***
B cells
cell number * 10^7
**
T cells
cell number * 10^7
ctrl
LMP1/CD30
B
ctrl
LMP1/CD30
250µm
C
ctrl
LMP1/CD30
IgM
IgD
14.3 ± 2.7
77.1 ± 4.2
20.1 ± 5.1*
69.7 ± 9.9
CD21
CD23
4.9 ± 1.5
81.5 ± 1.3
10.4 ± 3.4
5.9 ± 1.7
63.1 ± 11.0*
24.2 ± 10.4**
CD43
CD23
3.6 ± 0.9
76.4 ± 2.4
18.9 ± 2.5****
54.7 ± 7.0****
CD5
B220
2.5 ± 1.0
85.7 ± 5.2
5.7 ± 0.9
3.8 ± 1.5
71.0 ± 15.1*
14.4 ± 7.4*
D
B1a
B1b
B2
cells * 10^6
**
***
ns
ctrl
LMP1/CD30

Figure 2

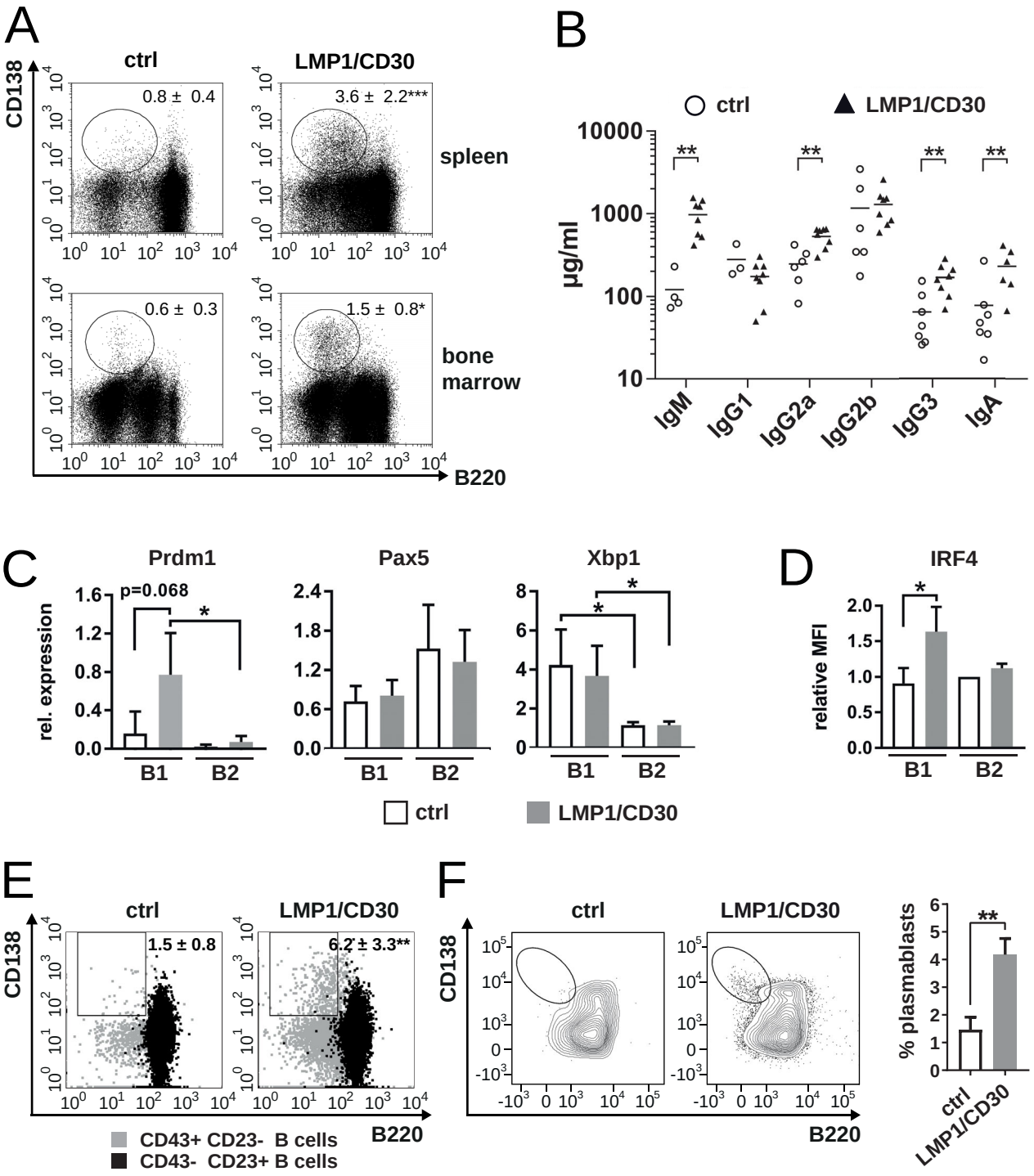
A
ctrl
LMP1/CD30
CD138
B220
0.8 ± 0.4
3.6 ± 2.2***
0.6 ± 0.3
1.5 ± 0.8*
spleen
bone marrow
B
ctrl
LMP1/CD30
µg/ml
IgM
IgG1
IgG2a
IgG2b
IgG3
IgA
C
Prdm1
Pax5
Xbp1
rel. expression
p=0.068
B1
B2
ctrl
LMP1/CD30
D
IRF4
relative MFI
E
1.5 ± 0.8
6.2 ± 3.3**
CD43+ CD23- B cells
CD43- CD23+ B cells
F
% plasmablasts

Figure 3

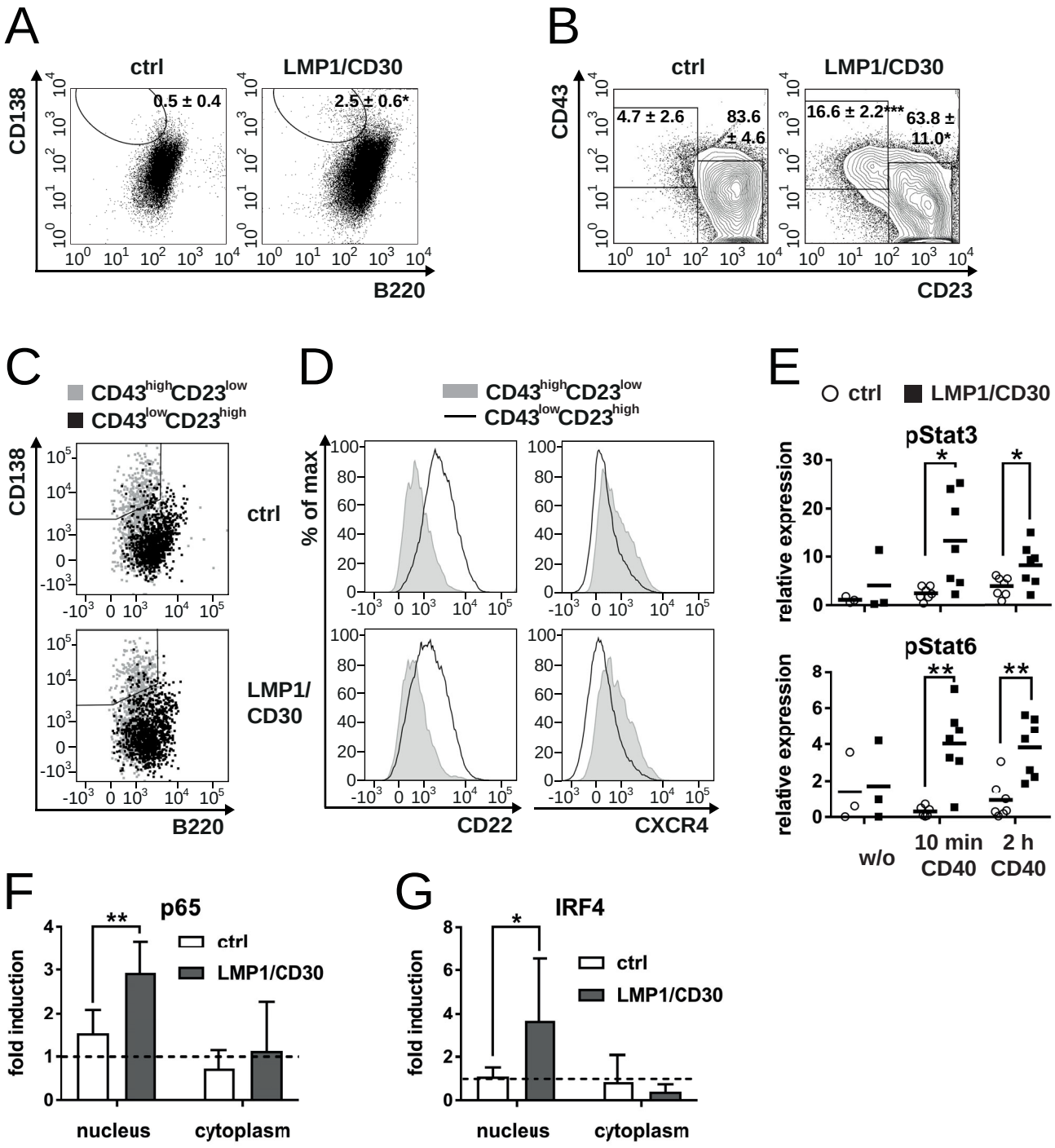
A
ctrl
LMP1/CD30
CD138
B220
0.5 ± 0.4
2.5 ± 0.6*
B
ctrl
LMP1/CD30
CD43
CD23
4.7 ± 2.6
83.6 ± 4.6
16.6 ± 2.2***
63.8 ± 11.0*
C
CD43highCD23low
CD43lowCD23high
CD138
B220
ctrl
LMP1/CD30
D
CD43highCD23low
CD43lowCD23high
% of max
CD22
CXCR4
E
ctrl
LMP1/CD30
pStat3
pStat6
relative expression
w/o
10 min CD40
2 h CD40
F
p65
ctrl
LMP1/CD30
fold induction
nucleus
cytoplasm
G
IRF4
ctrl
LMP1/CD30
fold induction
nucleus
cytoplasm

Figure 4

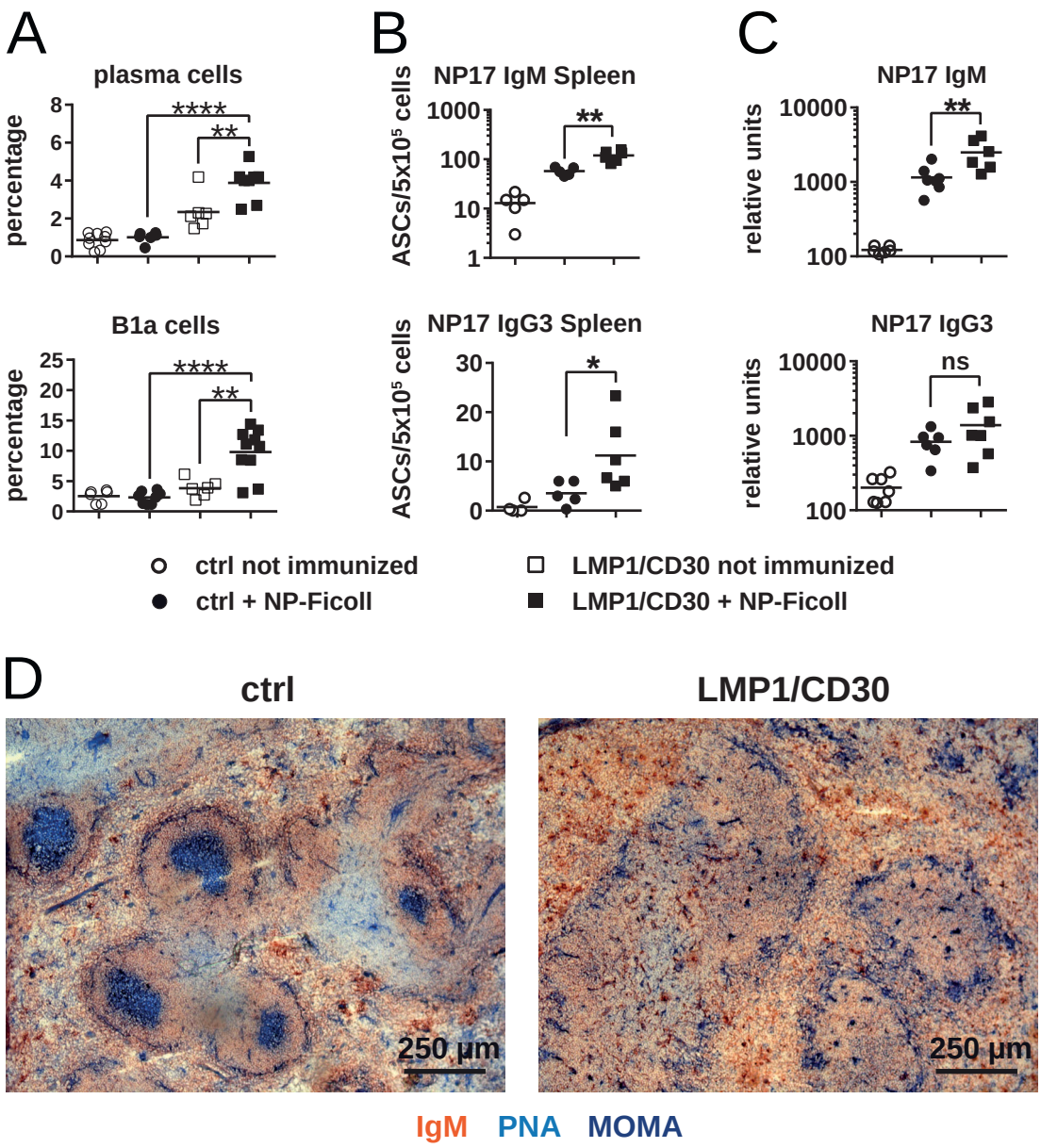
A
plasma cells
percentage
****
**
B1a cells
percentage
****
**
B
NP17 IgM Spleen
ASCs/5x10⁵ cells
**
NP17 IgG3 Spleen
ASCs/5x10⁵ cells
*
C
NP17 IgM
relative units
**
NP17 IgG3
relative units
ns
ctrl not immunized
ctrl + NP-Ficoll
LMP1/CD30 not immunized
LMP1/CD30 + NP-Ficoll
D
ctrl
LMP1/CD30
250 µm
250 µm
IgM PNA MOMA

Figure 5

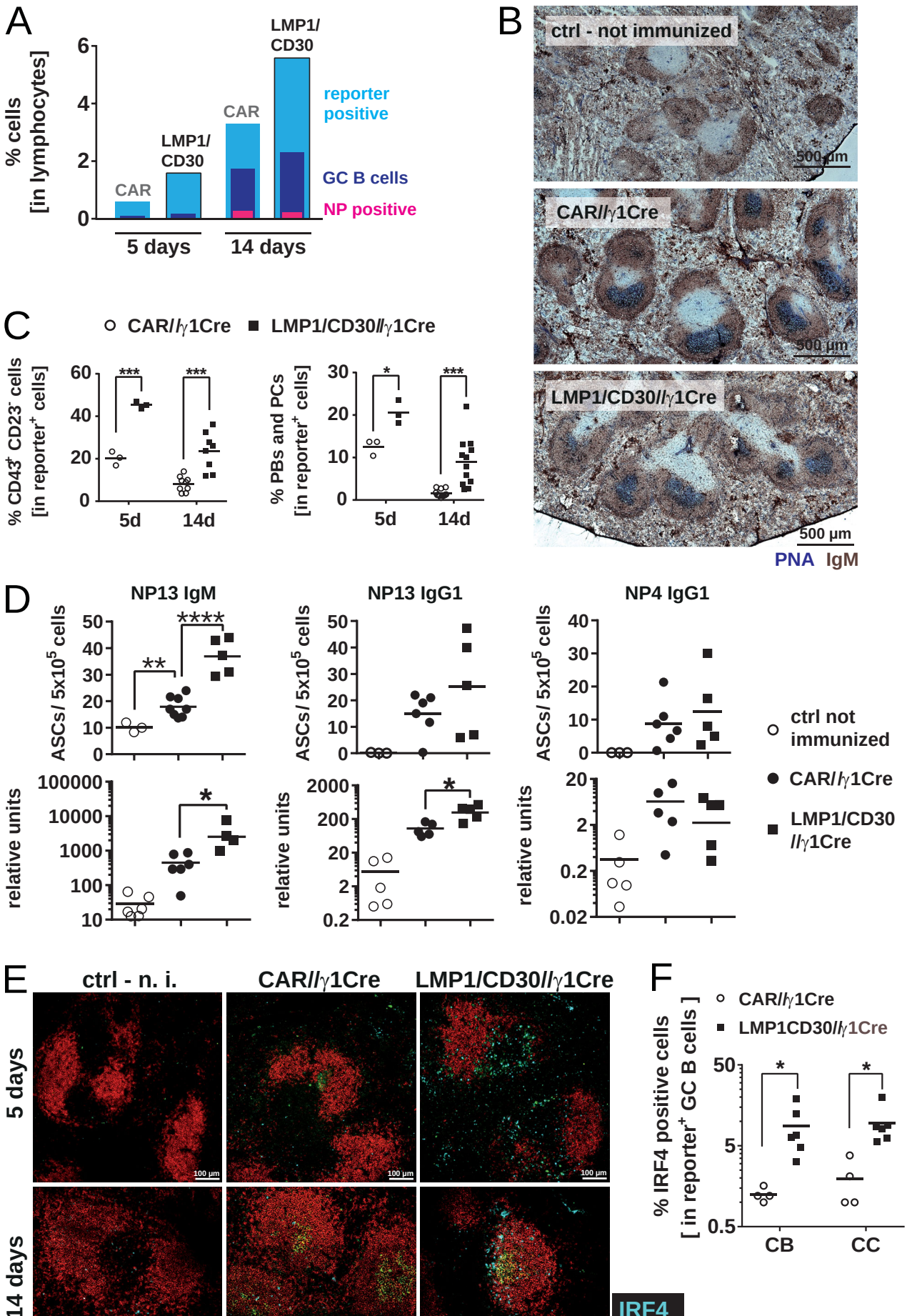
A
% cells [in lymphocytes]
6
4
2
0
CAR
LMP1/ CD30
CAR
LMP1/ CD30
reporter positive
GC B cells
NP positive
5 days
14 days
B
ctrl - not immunized
500 µm
CAR/Iγ1Cre
500 µm
LMP1/CD30/Iγ1Cre
500 µm
PNA IgM
C
CAR/Iγ1Cre
LMP1/CD30/Iγ1Cre
% CD43+ CD23- cells [in reporter+ cells]
60
40
20
0
***
***
5d
14d
% PBs and PCs [in reporter+ cells]
30
20
10
0
*
***
5d
14d
D
NP13 IgM
NP13 IgG1
NP4 IgG1
ASCs/ 5x10^5 cells
50
40
30
20
10
0
**
****
*
relative units
100000
10000
1000
100
10
2000
200
20
2
0.2
40
30
20
10
0
20
2
0.2
0.02
ctrl not immunized
CAR/Iγ1Cre
LMP1/CD30 /Iγ1Cre
E
ctrl - n. i.
CAR/Iγ1Cre
LMP1/CD30/Iγ1Cre
5 days
14 days
100 µm
IRF4
B220
GL7
F
CAR/Iγ1Cre
LMP1CD30/Iγ1Cre
% IRF4 positive cells [in reporter+ GC B cells]
50
5
0.5
*
*
CB
CC

Figure 6

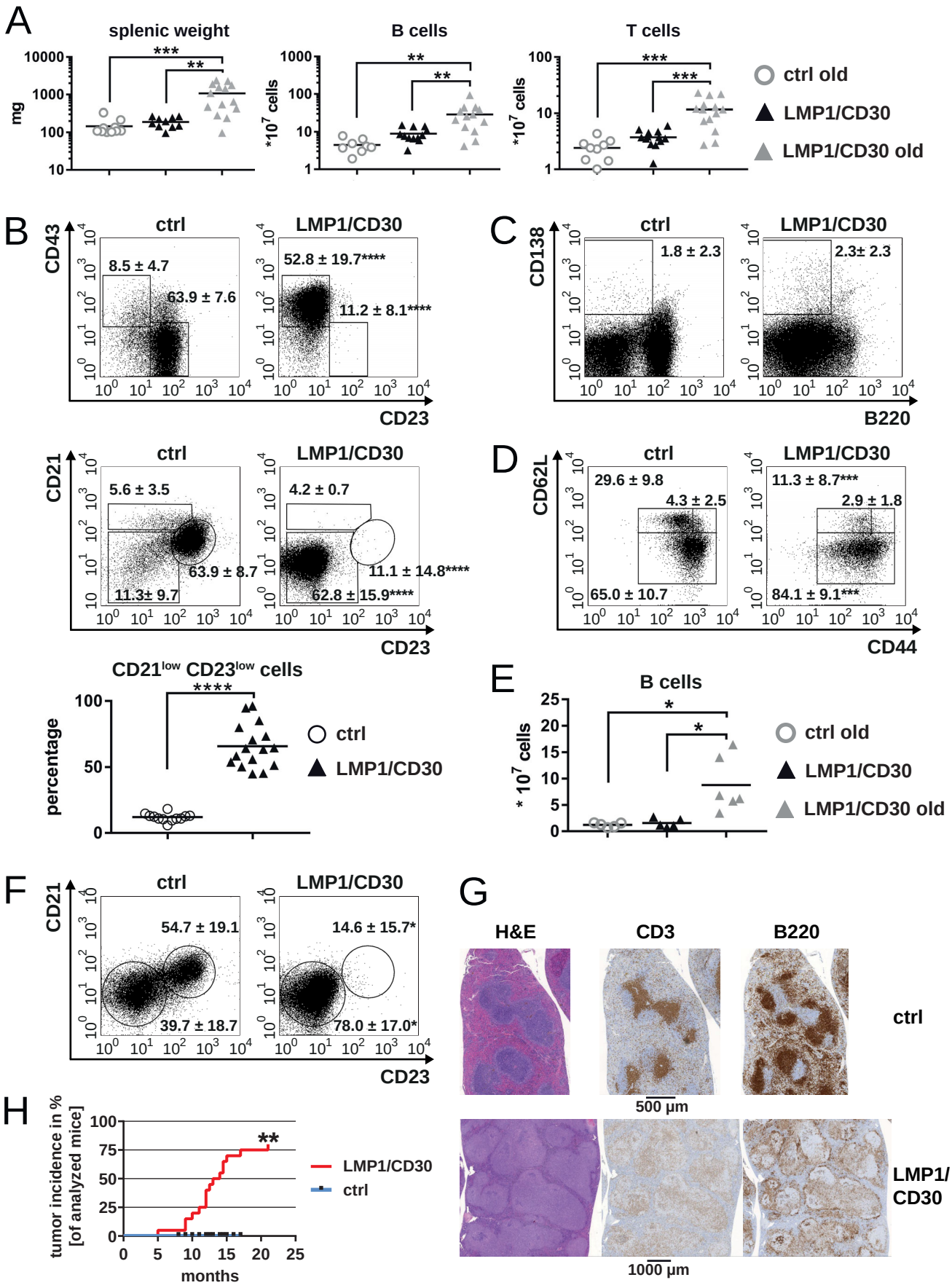
A
splenic weight
mg
B cells
*10^7 cells
T cells
*10^7 cells
ctrl old
LMP1/CD30
LMP1/CD30 old
B
ctrl
LMP1/CD30
CD43
8.5 ± 4.7
63.9 ± 7.6
52.8 ± 19.7****
11.2 ± 8.1****
CD23
C
CD138
1.8 ± 2.3
2.3± 2.3
B220
CD21
5.6 ± 3.5
63.9 ± 8.7
11.3± 9.7
4.2 ± 0.7
11.1 ± 14.8****
62.8 ± 15.9****
CD23
D
CD62L
29.6 ± 9.8
4.3 ± 2.5
65.0 ± 10.7
11.3 ± 8.7***
2.9 ± 1.8
84.1 ± 9.1***
CD44
CD21low CD23low cells
percentage
ctrl
LMP1/CD30
E
B cells
* 10^7 cells
ctrl old
LMP1/CD30
LMP1/CD30 old
F
ctrl
LMP1/CD30
CD21
54.7 ± 19.1
39.7 ± 18.7
14.6 ± 15.7*
78.0 ± 17.0*
CD23
G
H&E
CD3
B220
ctrl
500 µm
LMP1/CD30
1000 µm
H
tumor incidence in % [of analyzed mice]
months
LMP1/CD30
ctrl

Figure 7